Supplementary Information

Decoding the role of mycobacterial lipid remodelling and membrane dynamics in antibiotic tolerance

Anjana P. Menon[a,b,c], Tzong-Hsien Lee[b,c], Marie-Isabel Aguilar[b,c*], Shobhna Kapoor[a,b*]

[a]*Department of Chemistry, Indian Institute of Technology Bombay, Mumbai 400076, India*

[b]*IITB-Monash Research Academy, Indian Institute of Technology Bombay, Mumbai 400076, India*

[c]*Department of Biochemistry & Molecular Biology, Monash University, Clayton, VIC 3800, Australia*

This SI files contains 6 SI figures and Experimental Section

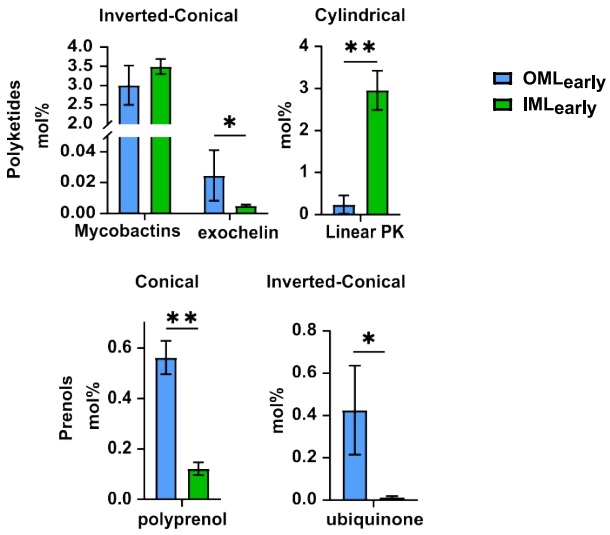

Figure S1. Abundance of polyketides and prenols across the mycobacterial membrane envelope in the early-stage infection.

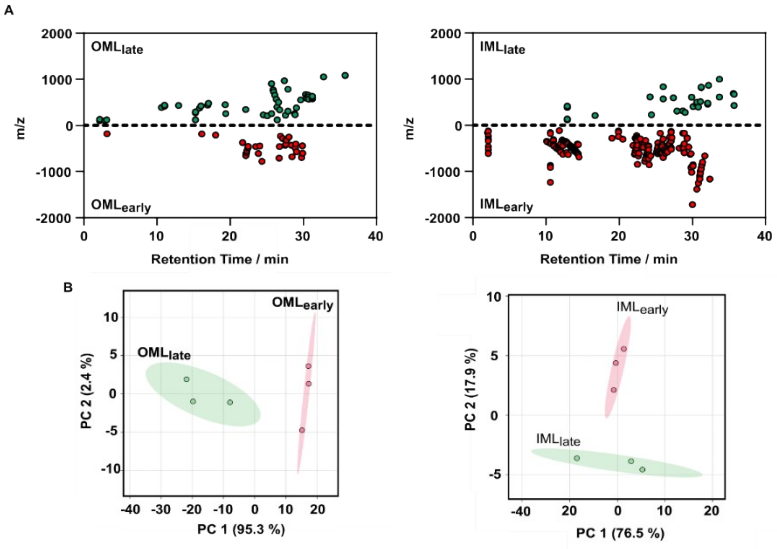

Figure S2. A). Cloud plot distribution of lipid detected in the mycobacterial membrane layers: green and red denotes individual lipids of at least 5-fold abundance in IML_{late} or IML_{early} regions, respectively. B). PCA score plot indicating extreme variation (~20 times) of PC1 (glycerophospholipids) in OML and (~5 times) of PC2 (saccharolipids) in IML lipid mixtures.

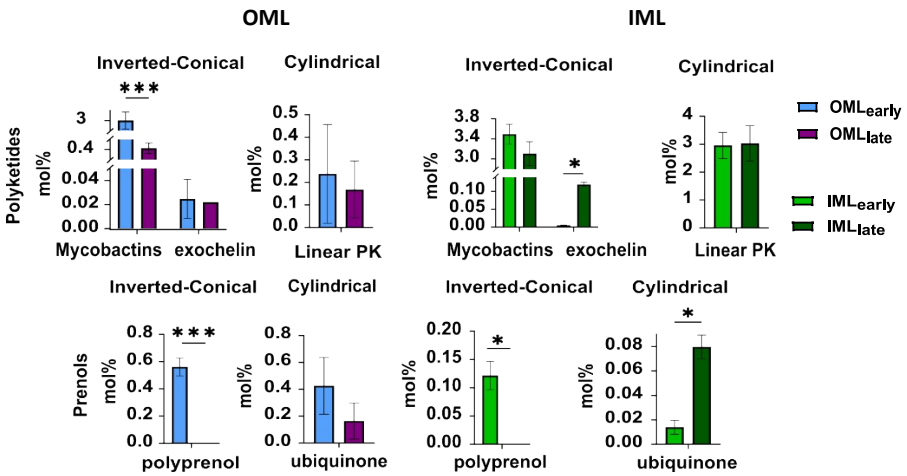

Figure S3. Variations in the abundance of polyketides and prenols in the OML and IML during early and late infections.

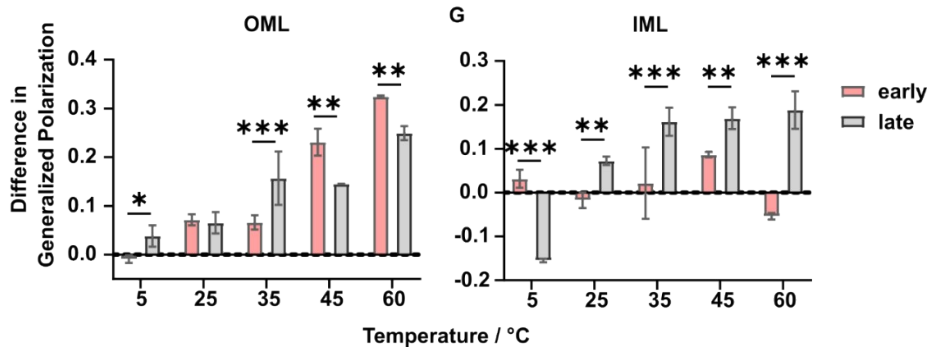

Figure S4. Difference in the Laurdan generalized polarization upon 10 mol% rifabutin addition to F). OML, G). IML, at different growth stages.

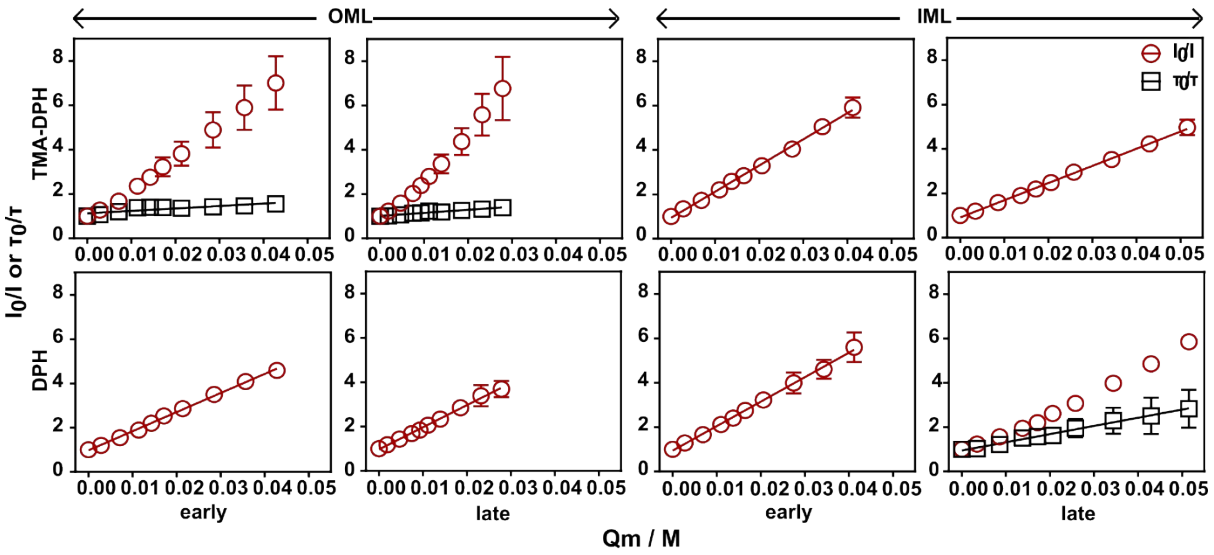

Probe	Lipid	Growth stage	Ksv (M^{-1})	Y-intercept	R^2	KD (M^{-1})	τ0 (ns)	KQ x 10^{10} (M^{-1} s^{-1})
TMA-DPH	OML	0.8 OD	90.33 ± 2.46	1.040 ± 0.055	0.994	11.01 ± 2.16	0.99 ± 0.03	9.12 ± 0.27
	IML		118.08 ± 2.09	0.938 ± 0.045	0.998	-	2.64 ± 0.18	4.47 ± 0.30
	OML	3.0 OD	104.20 ± 3.43	1.063 ± 0.050	0.991	13.89 ± 0.99	0.89 ± 0.04	11.69 ± 0.54
	IML		77.45 ± 1.15	0.911 ± 0.031	0.998	-	2.55 ± 0.19	3.03 ± 0.22
DPH	OML	0.8 OD	86.46 ± 1.40	0.974 ± 0.031	0.998	-	0.42 ± 0.09	20.79 ± 4.37
	IML		110.27 ± 1.69	0.942 ± 0.037	0.998	-	1.61 ± 0.09	6.87 ± 0.31
	OML	3.0 OD	99.96 ± 1.86	0.968 ± 0.027	0.997	-	1.34 ± 0.26	7.43 ± 1.44
	IML		20.89 ± 0.45	1.007 ± 0.012	0.996	36.94 ± 1.15	1.47 ± 0.16	1.42 ± 0.15

Figure S5. Rifabutin-driven quenching of DPH and TMA-DPH fluorescence intensity (I) and lifetime (τ) to determine its localization within the membrane. Table indicating the Stern-Volmer (static) (Ksv) and dynamic (K_D) quenching constant of the probe, Y-intercept and R^2 to indicate the goodness of fit, τ0 – fluorescence lifetime (ns) within different membranes, bimolar quenching constant (K_Q).

Experiments

1.1. Materials

Mycobacterium smegmatis (Msm) MC2 155 (ATCC), amikacin, moxifloxacin and clarithromycin were a humble gift Prof. Chopra (CDRI, Lucknow).

Product	Catalogue#	Company
2-Propanol	1.94524.2521	Sigma-Aldrich®
Acetic acid glacial	1.93402.0521	Emplura® Sigma-Aldrich®
Acetonitrile	1.00029.4000	LiChrosolv® Sigma-Aldrich®
acetylacetone	P7754	Sigma-Aldrich®
Albumin Bovine (BSA), Fraction V	0216006980	MP Biochemicals
Aluminium oxide basic (activity 1-II)	10072S500	Finar®
Ammonium acetate	09689	Sigma-Aldrich®
Anthrone	319899	Sigma-Aldrich®

AOT (Dioctyl sulfosuccinate sodium salt)	323586	Sigma-Aldrich®
Catalase from bovine liver	C9322	Sigma-Aldrich®
Chloroform	1.94506.2521	Emplura® Sigma-Aldrich®
DMSO	1.16743.0521	Emplura® Sigma-Aldrich®
DPH (1,6-Diphenyl-1,3,5-hexatriene)	D208000	Sigma-Aldrich®
Ethanol	1170	Changshu Hongsheng Fine Chemical Co. Ltd.
Formic acid	405823	Carlo Erba
glycerol	1.07051.0521	Emparta® Sigma-Aldrich®
Hydrochloric acid ~37%	1.93001.0521	Emparta® Sigma-Aldrich®
Laurdan (6-dodecanoyl-N,N-dimethyl-2-napthalmine)	40227	Sigma-Aldrich®
Methanol	1.07018.2521	Emparta® Sigma-Aldrich®
$MgCl_2.6H_2O$	M2393	Sigma-Aldrich®
Middlebrook 7H10 Agar Base	M199	Himedia®
Middlebrook 7H9 Base	271310	Difco™
Middlebrook 7H9 Broth	271310	BD DIFCO™
Miller Luria Bertani Agar	M1151	Himedia®
MilliQ	-	Sigma-Aldrich®
NaOH pellets (low chloride)	1.93102.0521	Emparta® Sigma-Aldrich®
n-Heptane	1.07053.2521	Emparta® Sigma-Aldrich®
PBS pellets	18912.014	Gibco™
Resazurin sodium salt $C_{12}H_6NNaO_4$	B21187	Alfa Aesar, Thermo Fisher Scientific
Rifabutin	16468	Cayman Chemicals
Sodium periodate	311448	Sigma-Aldrich®
Sulfuric Acid ~98%	1.93000.0521	Emparta® Sigma-Aldrich®
TLC Silica gel 60 F_{254}	1.05554.0001	Merck Millipore
TMA-DPH (N,N,N-trimethyl-4-(6-phenyl-1,3,5-hexatrien-1-yl)-benzenaminium, 4-methylbenzenesulfonate)	17294	Cayman Chemicals
Triton-X-100	032063	Spectrochem
Trizma® base	T1503	Sigma-Aldrich®
Tyloxapol	R0090187	Curia Global, Inc.
α-Dextrose	158968	Sigma-Aldrich®

1.2. Bacterial Culture

Mycobacterium smegmatis MC^2155 (*Msm*) was grown in Middlebrook 7H9 medium supplemented with 10% (v/v) in-house prepared albumin-α-Dextrose-catalase (ADC), 0.1% tyloxapol and 0.5% glycerol under shaking conditions at 37°C and 120 rpm. Cells intended for harvesting at the logarithmic growth phase were cultured until reaching OD_{600} 0.8, while those for carbon-limited stationary phase were grown separately without tyloxapol until reaching OD_{600} 3.0, measured using a micro-spectrophotometer (BioPhotometer D30, Eppendorf). For antibiotic susceptibility testing, *Msm* cells at OD_{600} 3.0 were re-cultured without tyloxapol until reaching a secondary log phase (~OD_{600} 0.8).

1.3. Resazurin Cytotoxicity Assay

Resazurin serves as a widely utilized marker for cell viability assessment, characterized by its conversion to resorufin in live cells without compromising their health. In the OD_{600}-cell viability correlation assay, *Msm* cultures were harvested from media with and without tyloxapol at various time points spanning up to 35 hours. OD_{600} measurements were obtained using micro-spectrophotometer (BioPhotometer D30, Eppendorf), while cell viability was monitored using Multiskan SkyHigh plate reader (Thermo Fisher Scientific). For assessing *Msm* cell viability, 5 µL of 0.02% resazurin solution (filtered) was added to 100 µL of the harvested cells, followed by a 4-hour incubation period, with absorbance readings recorded at 570 nm and 600 nm.

For drug-cytotoxicity analysis, 100 µL of *Msm* diluted to 0.2 OD_{600} from either 0.8 OD_{600} or 3.0 OD_{600} cultures, was seeded in 96-well plate (SPL life sciences). Subsequently, 100 µL serial dilutions of antibiotics (0.004-200 µM) were added to each well in triplicate and thoroughly mixed. Positive (PC) and negative (NC) controls, consisting of 1% Tx100 and antibiotic-free cells, respectively, were included. The plate was then incubation at 37°C for 24 hours to facilitate drug-cell interaction. Following drug incubation, 5 µL of 0.02% resazurin solution was added to each well, and then the plate was further incubated for 7 hours to allow reduction to resorufin. Absorbance readings were subsequently recorded at 570 nm and 600 nm using CLARIOstar^{Plus} plate reader (BMG Labtech). The following equations was then used to monit`or the cell viability (eq. 01) and then relative cell viability (eq. 02).

$$\text{Cell viability} = \frac{\varepsilon_{OX_{570nm}} X\, A_{570nm_{tx}} - \varepsilon_{OX_{570nm}} X\, A_{600nm_{tx}}}{\varepsilon_{RED_{570nm}} X\, A_{600nm_{t0}} - \varepsilon_{RED_{600nm}} X\, A_{570nm_{t0}}} \quad \text{eq. 01}$$

$$\text{Relative Cell Viability} = \frac{Cell\,Viability_{sample} - Cell\,Viability_{PC}}{Cell\,Viability_{NC} - Cell\,Viability_{PC}} \quad \text{eq.02}$$

1.4. Determination of Glycerol Concentration

Glycerol content is determined my sequential conversion to a fluorescent molecule using two reagents. Reagent I, the periodate reagent, consisted of 18 mg/mL sodium periodate dissolved in distilled water with 10% (v/v) acetic acid and 77 mg/mL ammonium acetate. Reagent II, the acetylacetone reagent, was composed of 1% (v/v) acetylacetone in isopropyl alcohol which is to be stored in the dark. To 40 µL of sample (cell-free supernatant of the cell culture) in each well of 96 well plate (SPL life sciences), 40 µL Reagent I was added and mixed adequately (Malaprade reaction). After an incubation time of 10 min, 125 µL Reagent II was pipetted into each well and mixed adequately (Hantzsch reaction). The absorption at 410 nm was measured over a period of 25 min using a microplate reader (CLARIOstar^{Plus}, BMG Labtech). The glycerol content was calculated with eq. 03, based on a glycerol standard curve (50 -200 mg/mL) (**Fig. S6**).

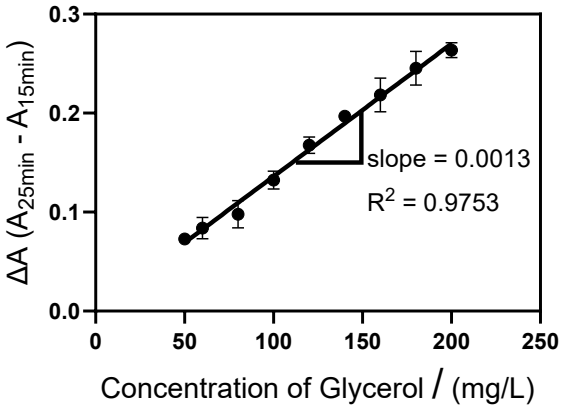

Figure S6. Standard curve of glycerol concentration ranging from 50-200 mg/L

$$\text{Glycerol content } [\frac{mg}{L}] = \frac{\Delta A_{sample(25min-15min)} - \Delta A_{blank(25min-15min)}}{slope\ of\ the\ calibration\ curve\ [\frac{L}{mg}]} \quad \text{eq. 03}$$

The glycerol content was correlated with the cells in the media with respect to the OD_{600}. 1.0 OD_{600} indicates $3.13x10^7$ CFU/mL and 0.4 OD_{600} indicates $1.97x10^6$ CFU/mL. The cell count from OD_{600} was derived by correlation and used in the following equation (eq. 04) to determine glycerol content per cell.

$$\text{Glycerol content } \left[\frac{\mu g}{mL}\right]/\text{cell} = \frac{Glycerol\ content\ \left[\frac{mg}{L}\right] X\ 1000}{\frac{CFU}{mL}\ at\ each\ OD_{600}} \quad \text{eq. 04}$$

1.5. Extraction of lipid

Mycobacterial lipids were extracted by the methods reported previously[1]. *Msm* cells were harvested at 5000g for 10 mins and the pellets were washed twice with phosphate buffer saline (pH 7.4) before lipid extractions. Non-covalent outer leaflet lipids of the Mycobacterial outer membrane (OML) were selectively extracted using 1 mL of reverse micellar solution (RMS; 10 mM AOT in heptane) for every 10 mg of dry weight of cells. For the inner membrane lipid (IML) extraction, the RMS-treated cells were washed twice with distilled water and then extracted with 3 mL of chloroform:methanol:water (2:1:0.1) for every 10 mg of dry mass. Both the extractions were carried out in monophasic solutions for four times, the first extraction spanning overnight and the rest for 30 minutes. The extracts were dried to obtain respective lipids.

OML extract was then purified from its AOT mixture using column chromatography of 100-200 alumina mesh with a mobile phase of gradient methanol in chloroform (up to 8%)[2][3][6][7][10][14]. Almost all lipids, with no AOT, get eluded at up to 8% methanol, which was confirmed from the fractions run on thin layered chromatography (TLC) developed by 1% anthrone spray.

1.6. Preparation of liposomes

Liposomal suspensions of different extracted lipids were prepared by hydration method. OML and IML were diluted in chloroform in the presence of lipid probes laurdan (0.5 mol%)/TMA-DPH (1 mol%)/DPH (0.5 mol%) to obtain a final lipid concentration of 0.5 mg/mL, unless stated otherwise. The lipid film was prepared by drying the chloroform under a stream of nitrogen gas followed by drying it under reduced pressure conditions overnight. For UV-Vis and fluorescence spectroscopy assays, the film was hydrated with 0.22 µm-filtered aqueous buffer (20 mM Tris, 5 mM $MgCl_2$, pH 7.4) at room temperature and was sonicated for 15 minutes, followed by five freeze-thaw cycles to generate large unilamellar vesicles (LUVs)[3]. For the drug-lipid membrane studies, anti-tubercular drug rifabutin was added in 10:1 lipid:drug molar ratio[4], unless specified otherwise and incubated for a period of 1 h in dark at 37 °C.

1.7. Liquid Chromatography

An Agilent 1260 HPLC (Agilent Technologies; Palo Alto, CA) with a 2.1 inner diameter (ID) × 150 mm, 3.5 µm XBridge C18 column (Waters Corp.; Milford, MA) heated to 45°C was used with a binary solvent system and a flow rate of 175 µl/min. The system was equilibrated with 95% solvent A [0.1% Formic acid in filtered MilliQ water] and 5% solvent B [0.1% formic acid in acetonitrile, and an aliquot of the lipid extract (5 µl = 20 µg dried extract) was applied to the column. This solvent gradient was maintained for 5 minutes followed by a 24 min. linear gradient to 100% Solvent B, and held at 100% for another 5 minutes.

1.8. Mass Spectrometry

An Agilent AdvanceBio 6545XT quadrupole time-of-flight (Q-TOF) mass spectrometer equipped with an Agilent ESI/atmospheric-pressure chemical ionization (APCI) multimode source was used for accurate mass analysis of the LC eluent. Positive(+) ion data were generated by operation of the mass spectrometer in ESI mode with a capillary voltage of 4000 V, nebulizer of 45 psig, drying gas of 8 l/min, gas temperature of 300 °C, vaporizer temperature of 300 °C, fragmentor of 175 V, charging voltage of 1000 V, skimmer of 65 V, and octopole radio frequency voltage of 750 V. Mass spectra were acquired in 4 GHz high-resolution mode at a rate of 1.0 spectra/s and 5882 transients/spectrum, and data were collected as profiled spectra over a mass range of 100 to 3,200 Da. Mass calibration was performed with an Agilent tune mix from 100 to 3200 Da, and an external reference sprayer introduced mass ions of m/z 922.009798 (+ ion) to enable accurate mass determinations. Data were collected with the Agilent MassHunter WorkStation Data Acquisition software, version B.10.00. An Agilent 6545 qTOF was used for MS/MS analyses of the compounds for confirmation. The instrument setup was the same as described above, with collision energies with slope of 6.5 V/100 Da and offset 2.0V were used for fragmentation.

1.9. Data Processing and Analyses

Cloud plot analysis was conducted by comparing the complete compound analysis of each mixture. Each molecule was considered identical only if it appeared within the range of ±0.5 mDa m/z and ±0.1s RT. Molecular abundances showing at least a 5-fold upregulation or downregulation were tabulated in GraphPad Prism 10.2.0.

LC/MS data files were processed with the MassHunter Qualitative Analysis Software, version B.10.00 (Agilent Technologies; Santa Clara, CA). MFs were extracted from the raw data using the MF extraction (MFE) algorithm. This algorithm locates related covariant ions (isotopes and charge states) from accurate mass LC/MS data, and combines these ions into a single feature. The MFE parameters used were: extraction algorithm, small molecule; peak filters, 1000 counts; ion species, +H and H only; peak spacing tolerance, 0.0005 m/z plus 5.0 ppm; isotope model, common organic molecules; charge state, 1–2; compound filters, none; mass filters, none; and mass defect, none. The resulting MFs were then identified with MassHunter by compound screening by formulas derived from Mtb LipidDB and MycoMass database file with the following search parameters: values to match, mass only; match tolerance, 5 mDa; charge carriers, +H, -H; and charge state range, 1–2. From the list thus obtained, the quantitative abundance of each compound was derived by using the following formula.

$$\text{Concentration of lipids (ppm)} = \frac{area_{lipids}\, X\, concentration\ of\ reserpine\ (ppm)}{area_{reserpine}} \qquad \text{eq.05}$$

$$\text{Mol\% of lipids} = \frac{\frac{Conc._{lipids(ppm)} X\ 0.001}{MW_{Lipids}} X\ 100\%}{Total\ no.\ of\ moles} \qquad \text{eq. 06}$$

For Principal Component Analysis (PCA), the mol% were uploaded in MetaboAnalyst 6.0 in the Generic Format for Statistical Analysis (one factor), without normalization or any further processing of the data. The data reflects relative changes in the abundance of various lipids with growth stage assessed using reserpine as the standard.

1.10. Molar volume (V_m) determination

V_m of a known lipid mixture is determined by neutral buoyancy method based on previous studies [5, 6]. Different ratios of D_2O in H_2O were used as the solvent to hydrate the lipid films generating the liposome for this experiment. The mass fraction of D_2O (ϕ_{D2O}) in the solvent was determined by the following equation.

$$\varphi_{D_2O} = \frac{m_{D_2O}}{m_{D_2O} + m_{H_2O}} \qquad \text{eq. 07}$$

where m_{D2O} and m_{H2O} represents the mass D_2O and H_2O respectively.

The inverse density of the final solvent (V_{sol}) can then be obtained by the following equation.

$$V_{sol} = \frac{\varphi_{D_2O}}{\rho_{D_2O}} + \frac{(1 - \varphi_{D_2O})}{\rho_{H_2O}} \qquad \text{eq. 08}$$

where ρ_{D2O} and ρ_{H2O} represents the densities of D_2O and H_2O respectively at 25 °C.

Assuming the interlamellar solvent and the bulk solvent are the same after liposome preparation, and following the principle that LUVs sink when suspended in a solution with lower density that the lipids and float in a higher density solution, the specific volume (V_S) of the lipids will fall within the range of solutions in which they float and sink.

Liposomal suspensions prepared from a broad range of V_{sol} (V_A and V_B) were centrifuged at 19800 g for 30 minutes at 25 °C. The liposomes were visually checked to determine whether they have sunk or floated. This range was narrowed and centrifuged until it reached V_A-V_B=0.01 mL/g (where the liposomes sink in V_A, and float in V_B), thereby determining the V_S within ±0.005 mL/g. The obtained V_S is the average of the final V_A and V_B.

The procedure was validated by deriving the specific volume of DPPC to be 0.941 mL/g, compared to the reported value of 0.94 mL/g at 25 °C. From the theory of neutral buoyancy method, the following equation can be derived.

$$V_m = V_S\, x\, MW \qquad \text{eq. 09}$$

where MW represents the equivalent molecular weight of the lipid mixtures.

1.11. Partition coefficient (K_P) determination

The partition coefficient of rifabutin between the lipid membranes and the aqueous buffer was determined using a UV-visible derivative spectrometry[4, 7-9]. This technique has the advantage of not requiring the physical separation of free and membrane-bound drug molecules when sufficient lipid concentrations are considered [10]. The isosbestic points obtained from derivative spectrometry indicate that the drug has completely partitioned into both water and lipid phases, thereby eliminating the noise due to scattering [11].

Absorption of UV light by varying concentrations of liposomes (0-1000 µM), with and without the addition of 25 µM rifabutin after the aforementioned incubation, was measured at RT using Thermo Scientific™ Evolution™ 201/220 UV-Visible spectrophotometer. The intensities were then processed to obtain the third derivative with respect to the wavelengths using nprot Kp calculator. The third derivative intensities ranging from 284 nm – 297 nm were considered for each lipid system to calculate the K_P values by fitting the experimental data to the following equation using non-linear regression with Origin 2019b.

$$D_T = D_W + \frac{(D_m - D_w)K_p[L]V_m}{1 + K_p[L]V_m} \quad \text{eq. 10}$$

$$D = \frac{d^3abs}{d\lambda^3}$$

where D represents the third derivative intensity ( ) obtained from the absorbance of total rifabutin concentration (D_T), rifabutin distributed in lipid membrane phase (D_m) and rifabutin distributed in the aqueous phase (D_w); [L] is the molar lipid concentration and V_m is the molar volume derived earlier for each lipid mixtures.

1.12. Drug location in membranes

The extent of quenching experienced by the fluorescent probes, DPH (ex: 357 nm, em: 430 nm), positioned near the acyl chains, and TMA-DPH (ex: 355 nm, em: 430 nm), positioned closer to the polar head groups, in the presence of rifabutin, indicates the location of the drug on the membrane bilayers as it gets across the membrane systems [12-16].

Rifabutin at a concentration range of 0-30 µM was added to DPH/TMA-DPH tagged liposomal solutions, followed by an incubation in the dark for 20 minutes. The fluorescence intensities emitted by the probes were recorded at 37 ± 0.1 °C using Varian Cary Eclipse Fluorescence Spectrophotometer. For lifetime quenching studies, a 375 nm laser excitation source was used. The fluorescence lifetime decay was measured using a picosecond pulsed diode laser-based Time Correlated Single Photon Counting (TCSPC) system from IBH, UK with a repetition rate of 1 MHz, a full width half maximum (FWHM) of the instrument response function (IRF) of ~270 ps, and a photomultiplier tube (PMT) as the detector. The fluorescence lifetime decay spectra were fit using v6.2 IBH DAS software through an iterative reconvolution method with the χ^2 value ranging from 1-1.2. The lifetime contributions after fitting and the intensities at 430 nm obtained from spectrofluorometer were utilised to determine the patterns of quenching using either Stern-Volmer or modified Stern-Volmer equations[4] using GraphPad Prism10.

Considering the Kp of rifabutin for each membrane system, only a portion of the drug partitions into the membranes. Hence to derive the linearity of the quenching of the probes, the effective concentration of the drug (Q_m) contributing to the quenching of the probes can be calculated using the following equation.

$$Q_m = \frac{K_P[Q]_T}{K_p\alpha_m + (1 - \alpha_m)} \quad \text{eq. 11}$$

where $[Q]_T$ represents the total rifabutin concentration and α_m represents the volume fraction of membrane phase.

$$\alpha_m = \frac{V_{mem}}{V_{water}}; \quad \text{eq. 12}$$

where

V_{mem} and V_{water} represent the volumes of the membrane and water phase, respectively. The fluorescence intensity of the probes could be quenched due to various molecular interactions, thus both static and dynamic quenching probabilities were considered. The Stern-Volmer equation used to determine the ability of the drug to quench the probes is:

$$\frac{I_0}{I} = 1 + K_{SV}[Q]_m$$ eq. 13

where I_0 and I are the steady-state fluorescence intensities with and without the drug, respectively, and K_{SV} is the Stern-Volmer constant.

A linear fit with goodness of fit (R^2) > 0.990 indicates the absence of dynamic quenching. If linearity is absent, a dynamic component is involved, which can be calculated using the modified Stern-Volmer equation given below.

$$\frac{\tau_0}{\tau} = 1 + K_D[Q]_m$$ eq. 14

$$\frac{I_0}{I} x \frac{1}{1 + K_D[Q]_m} = 1 + K_{SV}[Q]_m$$ eq. 15

where τ_0 and τ are the lifetimes with and without the drug, respectively, and K_D is the dynamic quenching constant. The resulting line with K_{SV} as the slope would be linear with a goodness of fit (R^2) > 0.990. K_{SV} indicates the static quenching effect imparted by the drug on the probes and can be further utilized to determine the bimolecular quenching constant (K_q), representing the effect of both static and dynamic quenching.

$$K_q = \frac{K_{SV}}{\tau_0}$$ eq. 16

1.13. Laurdan Generalized Polarization (GP) spectroscopy

The fluorescence intensities of a solvatochromic dye Laurdan (ex. 350 nm; em. 440 nm/490 nm)-incorporated lipid vesicles, with and without rifabutin, was recorded using temperature-controlled Varian Cary Eclipse Fluorescence Spectrophotometer, considering the range of temperature from 5 °C - 90 °C giving a period of 3 minutes for equilibration with an accuracy of ± 0.1°C.

The generic formula of $GP = \frac{I_{440\,nm} - I_{490\,nm}}{I_{440\,nm} + I_{490\,nm}}$, where I indicates the intensity at specified wavelengths, may not accurately reflect changes at the lipid head groups in LUVs containing complex lipid mixtures. Hence GP values were obtained from spectra after log-normal Laurdan spectral decomposition[17, 18]. Each Laurdan spectrum was treated as a superposition of two log-normal (LN) functions –representing the non-relaxed (blue channel) and the relaxed state (green channel).

The raw data at each temperature was converted to wavenumber format – with wavenumber on the x-axis and intensity corresponding to wavenumber ($I = I_\lambda * \lambda^2$; where I_λ is the intensity in wavelength scale and λ is the wavelength) on y-axis. The spectra obtained is normalized, baseline corrected and subjected to log-normal deconvolution using Origin 2019b, identifying two peaks corresponding to charge transfer (I_B for blue channel) and solvent relaxation (I_G for green channel) were determined. The GP curve was then plotted using the following formula.

$$GP = \frac{I_B - I_G}{I_B + I_G}$$ eq. 17

1.14. Statistics

All results are presented as mean ± standard error of the mean (SEM) for the indicated number of experiments (n=3). Statistical analyses were performed using GraphPad Prism 10.2.0 (GraphPad Software Inc). Differences were considered significant if $p < 0.033$.

References

1. Adhyapak, P., et al., *Dynamical organization of compositionally distinct inner and outer membrane lipids of mycobacteria.* Biophysical journal, 2020. **118**(6): p. 1279-1291.
2. Adhyapak, P., et al., *Dynamical Organization of Compositionally Distinct Inner and Outer Membrane Lipids of Mycobacteria.* Biophys J, 2020. **118**(6): p. 1279-1291.
3. Kapoor S, W.A., Denter C, Zhai Y, Markgraf J, Weise K, Opitz N, Winter R., *Temperature–pressure phase diagram of a heterogeneous anionic model biomembrane system: Results from a combined calorimetry, spectroscopy and microscopy study.* Biochimica et Biophysica Acta (BBA)-Biomembranes., 2011. **1808**(4): p. 1187-95.
4. Pinheiro, M., et al., *Differential Interactions of Rifabutin with Human and Bacterial Membranes: Implication for Its Therapeutic and Toxic Effects.* Journal of Medicinal Chemistry, 2013. **56**(2): p. 417-426.
5. Greenwood AI, T.-N.S., Nagle JF., *Partial molecular volumes of lipids and cholesterol.* Chemistry and physics of lipids., 2006. **143**: p. 1-10.
6. Wiener MC, T.-N.S., Wilkinson DA, Campbell LE, Nagle JF., *Specific volumes of lipids in fully hydrated bilayer dispersions.* Biochimica et Biophysica Acta (BBA)-Biomembranes., 1988. **938**(2): p. 135-42.
7. Alves AC, R.D., Horta M, Lima JL, Nunes C, Reis S. 2017 Aug 31;14(133):20170408., *A biophysical approach to daunorubicin interaction with model membranes: relevance for the drug's biological activity.* Journal of The Royal Society Interface., 2017. **14**(133).
8. Magalhães LM, N.C., Lúcio M, Segundo MA, Reis S, Lima JL. , *High-throughput microplate assay for the determination of drug partition coefficients.* nature protocols., 2010. **5**(11): p. 1823-30.
9. Pinheiro M, P.S., Silva AS, Nunes C, Reis S., *Evaluation of the effect of rifampicin on the biophysical properties of the membranes: significance for therapeutic and side effects.* International journal of pharmaceutics., 2014. **466**(1-2): p. 190-7.
10. Santos NC, P.M., Castanho MA., *Quantifying molecular partition into model systems of biomembranes: an emphasis on optical spectroscopic methods.* Biochimica et Biophysica Acta (BBA)-Biomembranes., 2003. **1612**(2): p. 123-35.
11. Omran AA, K.K., Takegami S, Kitade T, El-Sayed AA, Mohamed MH, Abdel-Mottaleb M., *Effect of phosphatidylserine content on the partition coefficients of diazepam and flurazepam between phosphatidylcholine–phosphatidylserine bilayer of small unilamellar vesicles and water studied by second derivative spectrophotometry.* Chemical and pharmaceutical bulletin., 2002. **50**(3): p. 312-5.
12. Fernandes MX, d.l.T.J., Castanho MA. 2002 Aug 1;307(1):1-2., *Joint determination by Brownian dynamics and fluorescence quenching of the in-depth location profile of biomolecules in membranes.* Analytical biochemistry., 2002. **307**(1): p. 1-12.
13. Denicola A, S.J., Radi R, Lissi E. , *Nitric oxide diffusion in membranes determined by fluorescence quenching.* Archives of biochemistry and biophysics., 1996. **328**(1): p. 208-12.
14. Moench SJ, M.J., Stewart DH, Dewey TG., *Fluorescence studies of the location and membrane accessibility of the palmitoylation sites of rhodopsin.* Biochemistry., 1994. **33**(19): p. 5791-6.
15. Ferreira H, L.M., de Castro B, Gameiro P, Lima JL, Reis S., *Partition and location of nimesulide in EPC liposomes: a spectrophotometric and fluorescence study. .* Analytical and bioanalytical chemistry., 2003. **377**: p. 293-8.
16. Neves AR, N.C., Amenitsch H, Reis S., *Effects of resveratrol on the structure and fluidity of lipid bilayers: a membrane biophysical study.* Soft matter., 2016. **12**(7): p. 2118-26.
17. Zorila B, B.M., Popescu AI, Radu M., *Log-normal deconvolution of laurdan fluorescence spectra—A tool to assess lipid membrane fluidity.* Romanian Reports in Physics, 2016. **68**(2): p. 702-12.
18. Bacalum M, Z.B., Radu M., *Fluorescence spectra decomposition by asymmetric functions: Laurdan spectrum revisited.* Analytical biochemistry., 2013. **440**(2): p. 123-9.